

## Isothermal Transformation Austenite-Ferrite in a P92 Steel

A. Hintze Cesaro<sup>1,2</sup>, M.I. Luppo<sup>1</sup>, C.A. Danón<sup>1</sup>

<sup>1</sup>National Atomic Energy Commission (CNEA), Buenos Aires, Argentina

<sup>2</sup>Instituto Sabato, UNSAM-CNEA, Buenos Aires, Argentina

*E-mail contact of main author: hintze@cnea.gov.ar*

**Abstract.** The Time-Temperature-Transformation (TTT) diagram of an ASTM A335 P92 steel (9CrMoWVNNb) has been established starting from an austenitization temperature of 1050 °C. Isothermal transformation was carried out at temperatures from 625 up to 750 °C taking 25 °C intervals, using a high resolution dilatometer. Only two state fields (i.e., austenite and ferrite + carbides) were observed, in full agreement with previous results on similar steels. A subset of large austenite grains, with sizes significantly exceeding the mean, was observed in all of the tested samples. At temperatures below the nose of the TTT diagram, prior austenite grain boundaries were made visible by decorating them with carbides precipitated at the early stages of the transformation. Carbide decoration allowed to have an accurate picture of the size distribution of austenite grains under the prescribed conditions of thermal cycle. Above the nose, prior austenite grain boundaries are hardly seen due to a drastic change in carbide precipitation mechanisms. At the same time, the ferrite nucleation and growth is markedly different in these two temperature regions; there is a gradual transition between these two extreme behaviors.

The dilatometric curves obtained at each temperature were fitted to the Kolmogorov-Johnson-Mehl-Avrami expression in order to extract kinetic information about the austenite-ferrite transformation. Fitting was accomplished so as to take into account the presence of the large austenite grains.

**Key Words:** P92, isothermal transformation, TTT diagram.

### 1 Introduction

9-12%Cr ferritic/martensitic steels are widely used in steam power plants due to its very good properties, such as creep behavior, toughness and corrosion resistance at high temperatures [1]. In particular, the T/P 92 steel was designed as a modification of the T/P 91 with a reduction of Mo and an addition of W and B. This steel grade is a candidate for many applications in Generation IV nuclear power plants due to its elevated working temperature (620°C), higher creep rupture strength, and better weldability that the T/P 91 [2].

Thus far, several studies have analyzed the tempered microstructure and creep behavior of this alloy [3-6]. Nevertheless, there is no information available about the isothermal decomposition of austenite of the T/P 92 grade.

In this work, the kinetics of isothermal decomposition of austenite and the resulting microstructures were studied. The Time Temperature Transformation (TTT) diagram was developed using a dilatometric technique. Additionally, the effect of the grain size distribution of the parent phase on the kinetics of the isothermal decomposition was analyzed within the Johnson-Mehl-Avrami-Kolmogorov approach.

## 2. Experimental

The studied alloy was an ASTM A335 P92 grade manufactured by Vallourec – Mannesmann (France) as rolled tubes in the standard metallurgical condition, i.e., normalized at 1060 °C, 20 minutes and tempered at 780 °C, 60 minutes. The chemical composition of the studied steel is shown in Table I.

TABLE I: CHEMICAL COMPOSITION OF THE STUDIED ALLOY IN WT. %.

Alloy	C	Cr	Mo	W	Si	V	Nb	N	Mn	Ni	Al	B
P92	0.13	8.72	0.38	1.63	0.24	0.20	0.06	0.05	0.46	0.17	0.01	0.002

Isothermal heat treatments cycles were performed with a high resolution quench dilatometer, Bähr DIL805A. The samples machined from the tube were cylinders 10 and 4 mm in length and diameter respectively.

Samples were austenitized for 30 minutes at 1050 °C and then rapidly cooled to the isothermal transformation temperature,  $T_{iso}$ . Isothermal heat treatments were performed in order to obtain a complete decomposition of austenite. Heating and cooling rates were  $1^{\circ}\text{C}\cdot\text{s}^{-1}$  and  $0.3^{\circ}\text{C}\cdot\text{s}^{-1}$  respectively. A complete scheme of the thermal cycle is presented in the Fig. 1.

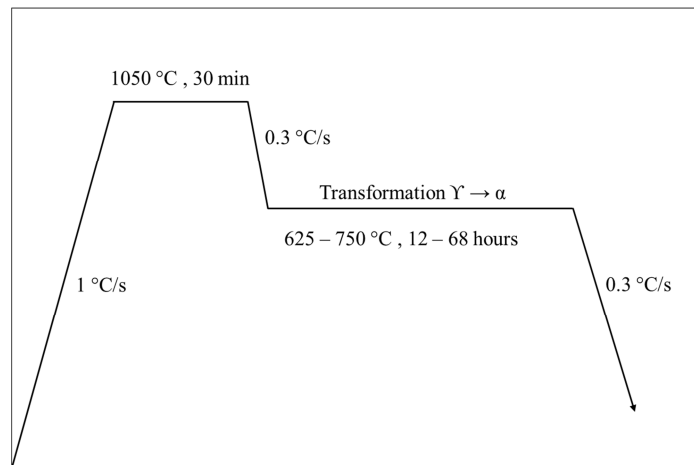


FIG. 1. Thermal cycle used for austenitization and further isothermal transformation to ferrite.

All isothermal cycles are detailed in Table II, transformation temperatures varied from 625 up to 750 °C taking 25 °C intervals and the holding times varied from 12 to 68 hours in order to obtain a fully transformed structure. Additionally an isothermal heat treatment for 12 hours at 625 °C, P1, was carried out in order to study the early stages of the austenite decomposition.

TABLE II: DETAILED ISOTHERMAL CYCLES FOR EACH SAMPLE.

Sample	F1	F2	F3	F4	F5	F6	P1	H3
Temperature [°C]	625	650	675	700	725	750	625	675
Time [hours]	68	30	12	12	12	12	12	4

After thermal cycles, samples were mounted in a conductive resin, grinded up to the mid plane, polished and etched with Vilellas's reagent to be examined by optical (OM). Grain size measurements were performed using an image analysis software. On the other hand, austenite grain boundaries of the "as received" condition were revealed using an electrolytic etching with oxalic acid.

Assuming a linear relationship between the sample change of length and the transformed fraction to ferrite, the extent of transformation  $\xi$ , was obtained as function of the dilatation vs time curves using the equation:

$$\xi = \frac{l - l_{min}}{l_{max} - l_{min}} \quad \text{eq 1}$$

where  $l_{min}$  and  $l_{max}$  are the minimum and maximum values of dilatation during the isothermal plateau and  $l$  is the length at a given time. Calculations were performed using as reference the A1033 – 04 ASTM standard. In order to study the dependence of the transformation rate with temperature, the extent of transformation versus time curves were analyzed with the empirical Johnson-Mehl-Avrami-Kolgomorov (JMAK) equation [7].

### 3. Results and Discussion

#### 3.1. Prior Austenite Microstructure

Fig. 2 shows OM and SEM micrographs of a sample transformed at 625°C for 12 hours (P1). This figure shows that at early stages of transformation, the  $\gamma \rightarrow \alpha$  reaction occurs exclusively along the ancient austenite grain boundaries. The ferrite nucleation and growth is accompanied with a carbide precipitation (in form of block, sphere, rod, and fibrous precipitates) that decorates the ancient austenite grain boundaries making them visible. Therefore, it was possible to have an accurate picture of the size distribution of austenite grains by observing the sample P1. It was assumed that the grain size distribution determined is representative of all samples since all heat treatment had the same austenitization cycle.

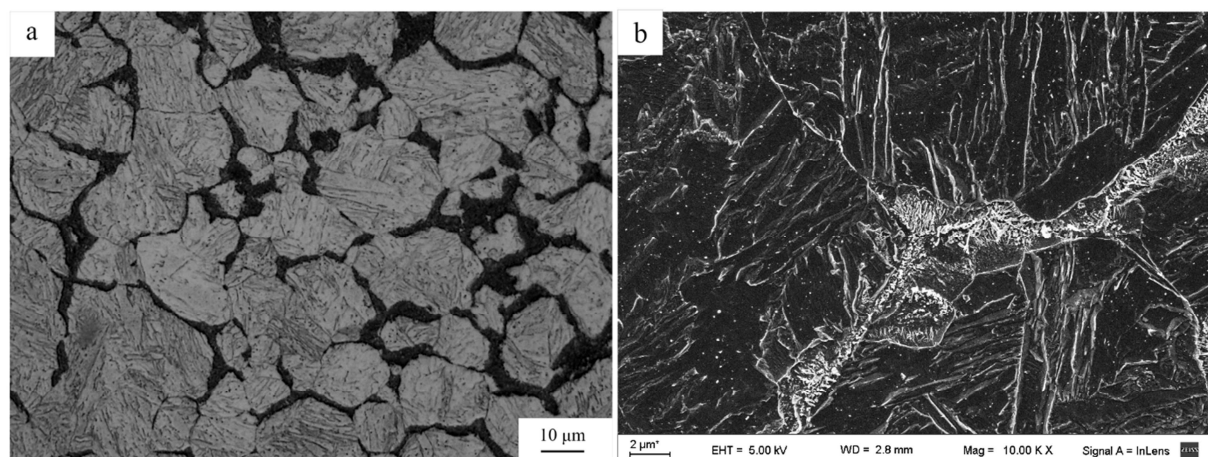


FIG. 2. Micrographs of the sample transformed at 625 °C for 12 hours (P1). (a) OM, (b) SEM..

Fig. 3 shows the austenite grain size distribution of the as received sample, Fig. 3(a), and the P1 sample, Fig. 3(b). It can be seen that the average grain size of the former is slightly lower than the latter. The austenite grains were divided in classes according to their size using the ASTM number, and the relative frequency was calculated as the number of grains per ASTM class divided the total amount of counted grains. In average, the "as received" condition has a

grain size diameter of  $12.9 \pm 0.3 \mu\text{m}$  meanwhile the austenite structure after the thermal cycle used in this work has an average diameter of  $17.8 \pm 0.2 \mu\text{m}$ .

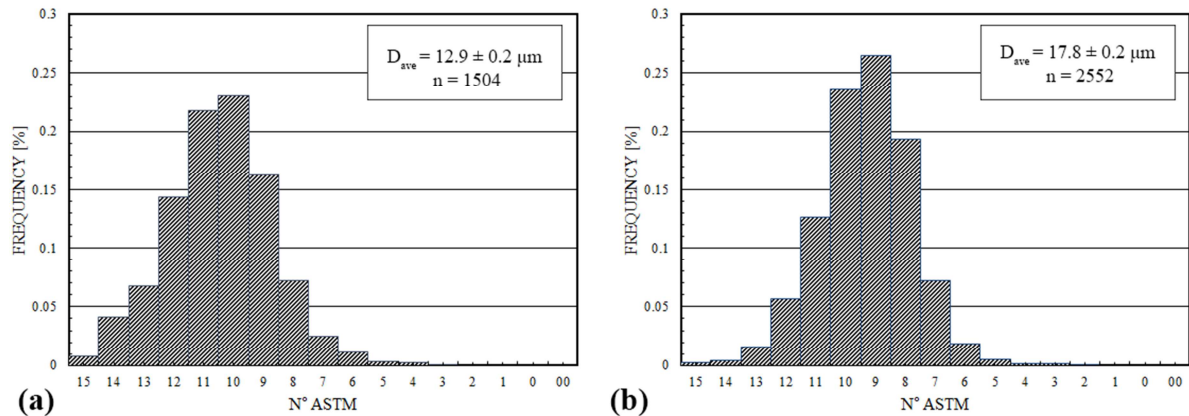


FIG. 3. Austenite grain size distribution: (a) as received sample, (b) P1 sample.

It is important to remark that both samples presented a small subset of grains with a size much larger than the rest. These grains are not observed in the histogram presented above since the amount of "large" grains compared to that of the "small" ones is very scarce, yet they represent a considerably fraction of the area observed in the sample.

Therefore, in order to remark the presence of this subset of grains with a size larger than the rest, instead of counting the number of grains per class (frequency counts) the relative area occupied by each class was determined and represented in Fig. 4.

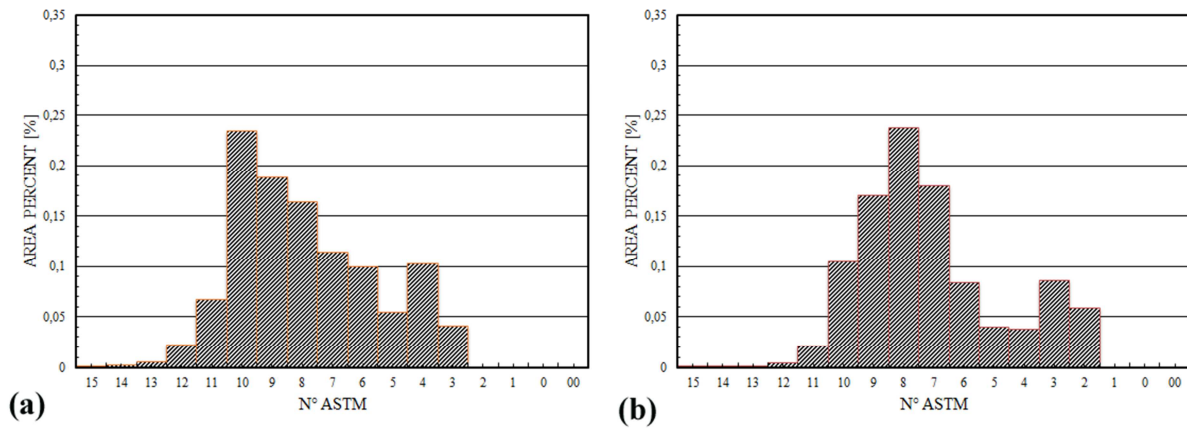


FIG. 4. Area % vs. ASTM number: (a) as received sample, (b) P1 sample.

The austenite grain size distribution seems to have heterogeneities in both conditions. Although the "as received" condition has a slightly smaller average grain size, both samples have a similar distribution. The assembly of small grains varied their size between 6 and 36 microns (i.e. N° ASTM "G" 11 – 6) with an average size of  $12.0 \pm 0.2 \mu\text{m}$  for the as received condition and  $16.9 \pm 0.2 \mu\text{m}$  for P1 condition. On the other hand, grains which experienced an abnormal grain growth reached mean diameters between 60 and 200 microns.

### 3.2. Kinetics of Isothermal Transformation

Isothermal kinetics of austenite decomposition in the temperature range 750 – 625 °C are presented in Fig 5(a). The extent transformation curves were determined from the dilatometric data using Eq. 1. From  $\xi$  vs.  $t$  curves, time values corresponding to 5, 50 and 99 % of transformation were used to plot the TTT diagram of Fig 5(b). It can be seen that the austenite decomposition rate is very sensitive to the transformation temperature and the maximum transformation rate is reached at 725 °C. At this temperature, transformation is completed after 4 - 5 hours of heat treatment. On the other hand, at 625 °C the transformation takes more than 60 hours to reach the 95% of transformed fraction.

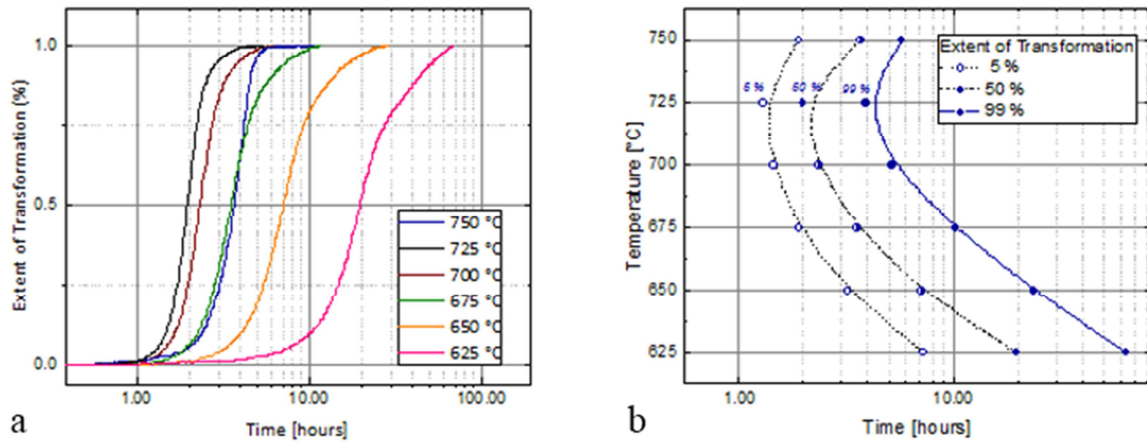


FIG. 5. (a) Extent transformation vs. time curves. (b) TTT diagram.

The conventional Avrami equation can be used to describe the overall transformation kinetics under isothermal conditions:

$$\xi = 1 - \exp\{-k(t - t_0)^n\} \quad \text{eq. 2}$$

where  $\xi$  is the volume fraction of austenite transformed to ferrite,  $t_0$  the onset or incubation time for the transformation,  $n$  the time exponent indicative of the transformation mechanism, and  $k$  is a temperature dependent factor. Equation 2 can be rewritten as:

$$\ln[-\ln(1 - \xi)] = n \cdot \ln(t - t_0) + \ln(k) \quad \text{eq. 3}$$

Assuming that Eq.3 describes the kinetics of this transformation, the  $n$  values at different temperatures are given by the slope of the  $\ln[-\ln(1 - \xi)]$  vs.  $\ln(t)$  plots.

Transformation versus time data sets were linearized and plotted in order to obtain the values of  $n$  for each transformation. For all transformation temperatures, except 750 °C, the  $\ln[-\ln(1 - \xi)]$  vs.  $\ln(t)$  plots presented **two linear regions with different slopes**, as shown in Fig. 6. Both slopes,  $n_1$  and  $n_2$  for each transformation are presented in Table III. On the other hand, only one slope was observed at 750°C, up to 98% of transformation.

The  $n_2$  slope is representative of the transformation up to approximately 70% of transformed fraction (i.e. for values of  $\ln[-\ln(1 - \xi)] < 0$ ). This time exponent increases with the transformation rate, reaching a maximum value at 725 °C. On the other hand,  $n_1$  represents the last stages of the transformation. The values calculated for  $n_1$  are remarkable lower than the ones calculated for  $n_2$ , and they also tend to grow with the transformation temperature.

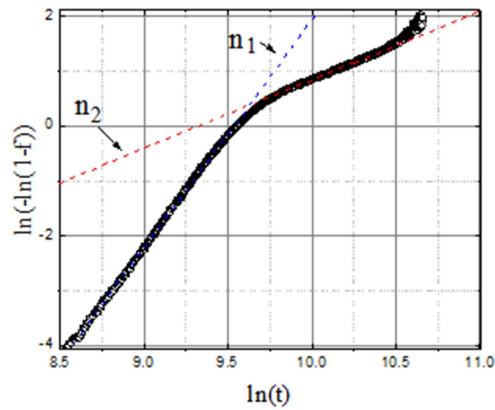


FIG. 6. Master curve for the transformation at 675 °C.

TABLE III: CALCULATED AVRAMI TIME EXPONENTS AT DIFFERENT TRANSFORMATION TEMPERATURES.

Temperature [°C]	$n_1$	$n_2$
625	1.18	2.75
650	1.14	3.26
675	1.25	4.16
700	1.53	5.45
725	1.66	6.35
750	4.76	

Johnson and Mehl [7] were the first to discuss the influence of the parent grain size distribution on the kinetic curves. They observed that the reaction curve for a steel with a “mixed” grain size structure would lie between those for the “large” and “small” grain sizes in the sample, but they also pointed out that the actual curve is not identical to the one calculated for the average grain size. Instead, the form of the actual curve will depend not only on the nature of the grain size distribution but also on the values of nucleation and grow rates.

Later, Matsuda et al. [8] adapted the Avrami’s classical transformation kinetics for a parent phase with a heterogeneous grain size distribution. The authors treated, with good experimental evidence, this case as a series of classes with uniform grain structure that transform independently from each other. Therefore, the overall transformation rate equation is obtained as the sum of different Avrami’s equations, one for each grain size category.

Particularly in heat resistant steels, Danon et al [9] showed that isothermal kinetic curves for the decomposition of austenite with a bimodal grain size distribution cannot be fitted with the standard Avrami’s equation. Instead, the combination of two equations, describing the kinetics for the assemblies of smaller and larger grains respectively, resulted in a good approximation to describe the transformation rate. The  $\ln[-\ln(1-\xi)]$  vs.  $\ln(t)$  plots revealed two different stages with different slopes, similar to the ones obtained in the present work.

The experimental curves obtained in this work are in good agreement with the expected behavior; transformation curves for each temperature do not show a fully sigmoidal shape and seem to be composed by the sum of different kinetic curves that represent the different grain size groups. Small grains react quickly and have a strong influence on the shape of the curve at early stages of the transformation, whereas the large grains will react slower affecting the later stages of the transformation. Nevertheless, it is important to remark that these curves are overlapped in time, so that the time exponents calculated in Table III do not necessarily represent the transformation mechanism of each group of grains. Experimental evidence of this behavior was obtained in sample H3. The H3 heat treatment was designed to obtain a half-fraction-transformed structure. It is observed that ferrite transformed exclusively in the small austenite grains Fig. 7 (a), so the larger ones have a fully martensitic structure after cooling at the end of the thermal cycle Fig. 7 (b).

The presence of two different slopes due to the deviation from the sigmoidal shape of the kinetic curve can be attributed to the presence of a parent phase with a heterogeneous grain size distribution. On the other hand, one possible reason to explain the unique time exponent  $n$  at 750 °C, resides on the fact that the nucleation rate at grain boundaries,  $N_S$ , and grow rate,  $G$ , are dependent on the transformation temperature. It is well known that at higher temperatures,  $N_S$  decreases and  $G$  increases, and therefore the  $N_S/G$  ratio decreases. According to Johnson and Mehl's work [7], the separation of transformation curves of given parent phases with different grain size distributions is greater when the  $N_S/G$  ratio increases. Thus, as temperature increases the evidence for the kinetic behavior due to a heterogeneous grain size distribution is more difficult to observe in both  $\xi$  vs.  $t$  or linearized curves since the portions associated to the small and large grains can be completely overlapped in time. Therefore, **the absence of two slopes cannot be directly related to a homogeneous grain size distribution.**

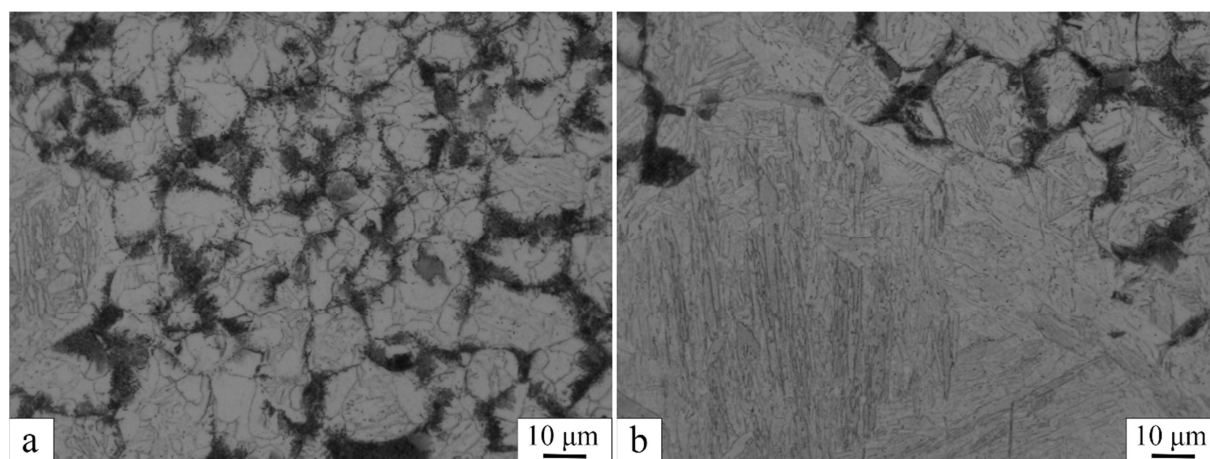
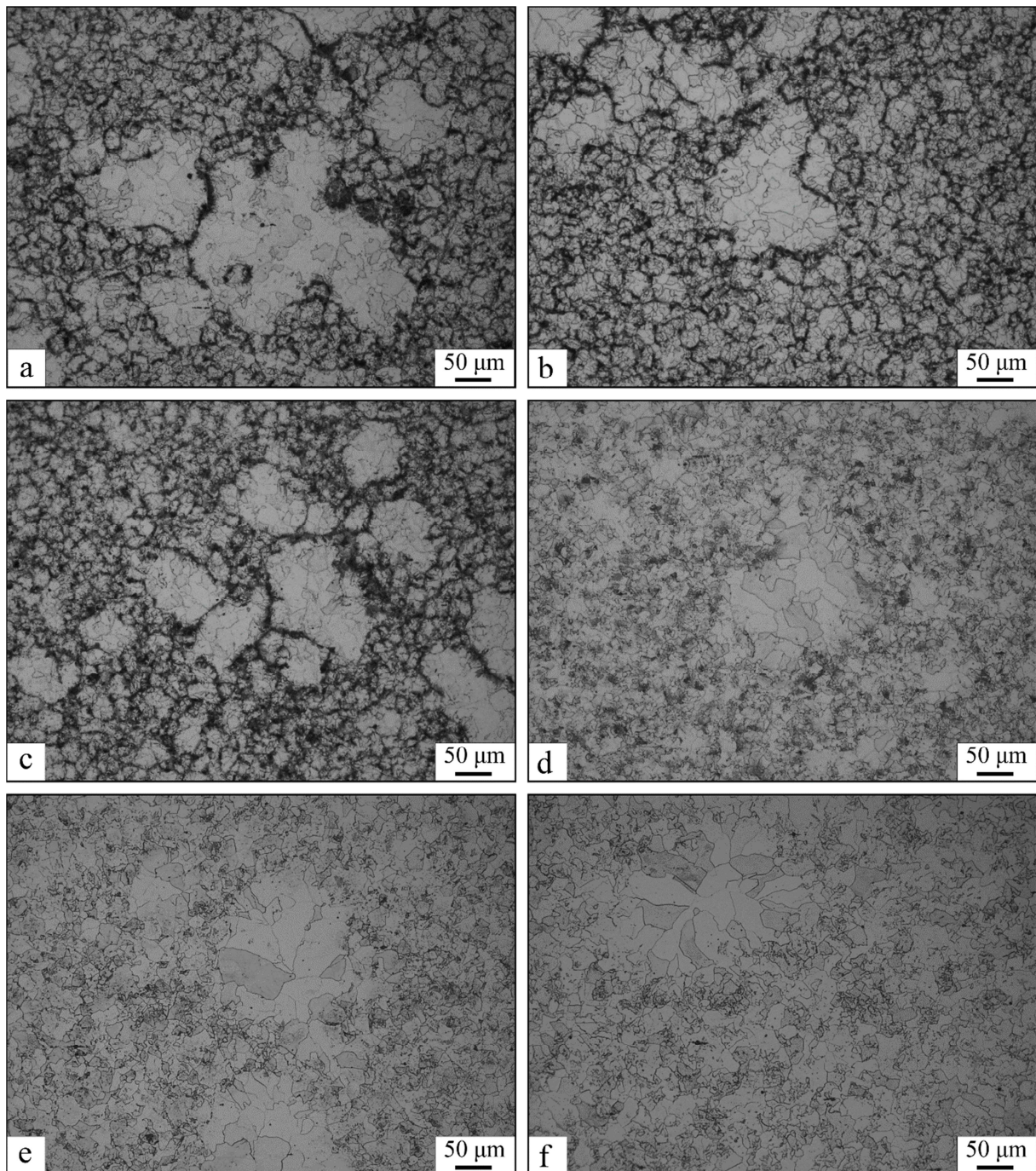


FIG. 7. Optical micrographs of two different areas of the same sample H3 treated for 4 hours at 675 °C. (a) Zone of small prior austenite grains. (b) Zone of large prior austenite grains.

### 3.3. General aspects of the microstructure of transformed samples

Fig. 8 shows the microstructure of fully transformed specimens after isothermal treatments. In all of the specimens it is clear that austenite decomposed to a ferritic matrix with an important fraction of precipitates,  $\gamma \rightarrow \alpha + \text{carbides}$ . The morphology and features of the precipitation varied significantly with the transformation temperature. At low temperatures a remarkable precipitation along all the prior austenite grain boundaries was clearly detected with OM. As

the transformation temperature increases the precipitation changes this particular feature and prior austenite grain boundaries are increasingly difficult to identify.



*FIG. 8. Optical micrographs of samples isothermally transformed into ferrite at different temperatures. (a) 625 °C, (b) 650 °C, (c) 675 °C, (d) 700 °C, (e) 725 °C, (f) 750 °C.*

As expected, the ferrite grain size was found to be dependent not only on the size of the parent austenite grain but also on the transformation temperature. At higher transformation temperatures, higher ferrite grain sizes were measured. To illustrate this behavior, the grain size distribution of ferrite grains having grown within abnormal austenite grains was determined for each temperature. Fig. 9 shows the corresponding histograms plotted for transformation temperatures of 625, 700 and 750 °C respectively. Although this Fig.

represents only the ferrite grains with an abnormal ( $> 50 \mu\text{m}$ ) parent austenite grain, this behavior was observed in all of the samples. It was chosen to plot only the subset of grains grown inside an abnormal austenite grain because of the remarkable relationship between the sizes of the mother and daughter phases. It can be seen in Fig. 9, that, for each temperature, the larger the austenite grain, the greater the size of the ferrite grains that grow inside

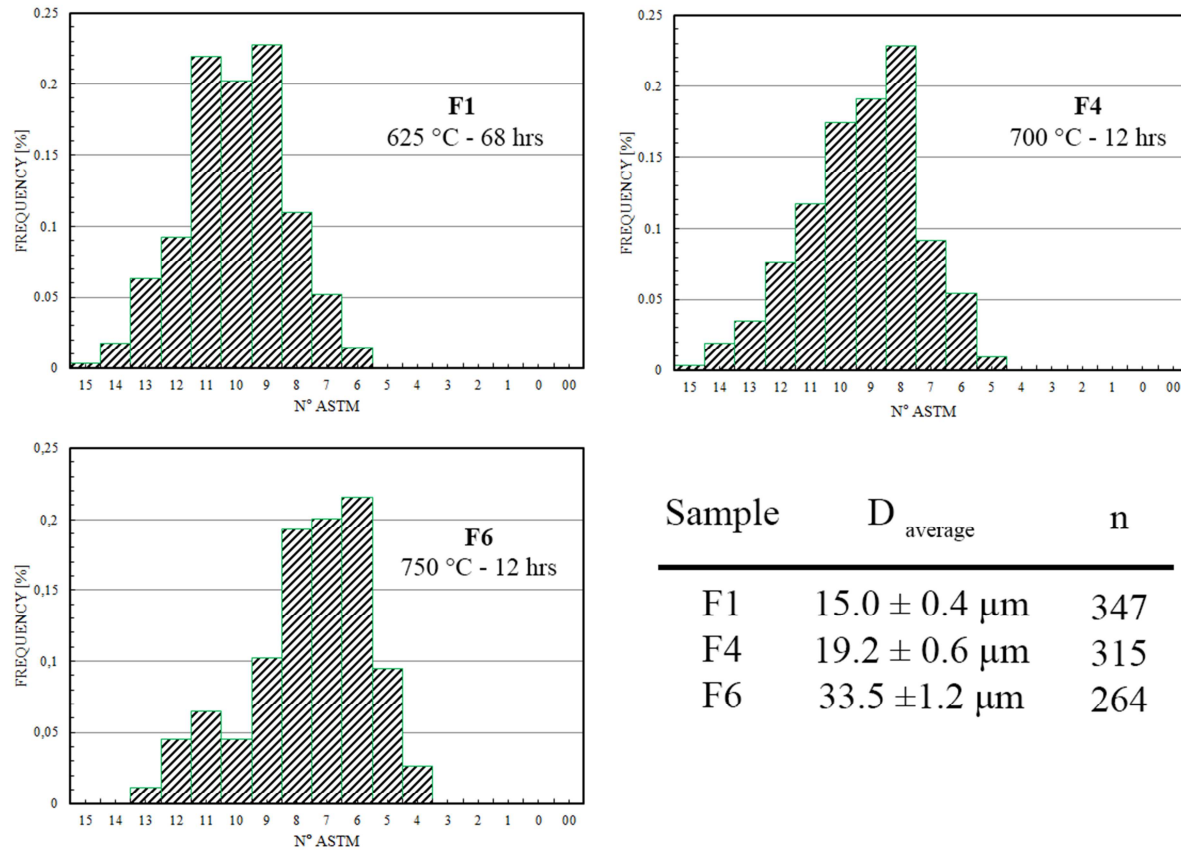


FIG. 9. Ferrite grain size distribution of the grains with an abnormal austenite parent grain for different transformation temperatures.

#### 4. Conclusions

The Time Temperature Transformation (TTT) diagram of an ASTM A335 P92 steel has been obtained by means of the dilatometric technique and the following conclusions can be drawn:

- At 725 °C the decomposition rate of austenite is maximum, taking less than 5 hours to transform completely into a ferrite and carbides structure.
- The microstructural features of the transformed (ferrite + carbides) structure are very sensitive to the transformation temperature. Two regions were clearly distinguished, with a gradual transition between them. At low transformation temperatures, carbides precipitate continuously along the ancient austenite grain boundaries at early stages of ferrite formation. At higher transformation temperatures, austenite grain boundaries become more difficult to distinguish since precipitation does not occur continuously along the grain boundaries.

- Austenite grain size distribution was found to be heterogeneous in both conditions studied (i.e., as received and heat-treated). Although similar distributions were observed after the austenitization step of the isothermal heat treatments and the commercial heat treatments, the prior austenite average grain size resulted smaller for the latter. Eventhough, “small” grains were observed to transform at early stages of the isothermal heat treatment, while “large” grains are the last ones to decompose to ferrite.
- Linearization of the JMAK equation revealed two transformation kinetic regimes. The slope change is believed to be a consequence of the heterogeneous austenite grain size distribution.
- The time exponent  $n$  is not necessarily correlated with the transformation mechanism of each subset of grains.

## 5. Acknowledgements

This work has been partially supported by grant PICT 2170-2014 from the Science and Technology Argentine Ministry.

## 6. References

- [1] ABE, F., “Precipitate design for creep strengthening of 9% Cr tempered martensitic steel for ultra-supercritical power plants”, *Sci. Tech. Adv. Mater.* **9** (2008) 013002.
- [2] ENNIS, P.J., et al., “Recent advances in creep resistant steels for power plant applications”, *OMMI* **1** (2002) 1.
- [3] SHEN, Y., et al., “Precipitate phases in normalized and tempered ferritic/martensitic steel P92”, *J. Nucl. Mat.* **465** (2015) 373.
- [4] SAKTHIVEL, T., et al., “Effect of thermal aging on microstructure and mechanical properties of P92 Steel”, *Trans. Indian Inst. Met.* **68** (2015) 411.
- [5] ISAAC SAMUEL, E., et al., “Creep deformation and rupture behavior of P92 steel at 923 K”, *Procedia Eng.* **55** (2013) 64.
- [6] NI, Y.Z., et al., “Study on creep mechanical behavior of P92 steel under multiaxial stress state”, *Mater. High Temp.* **32** (2015) 551.
- [7] JOHNSON, W.A., MEHL, R.F., “Reaction kinetics in processes of nucleation and growth”, *Trans. AIME* **135** (1939) 416.
- [8] MATSUDA, H., et al., “Avrami theory for transformations from non-uniform austenite grain structures”, *Mat. Sci. Tech.* **19** (2003) 1330.
- [9] DANON, C.A., et al., “Kinetics of the austenite-ferrite isothermal phase transformation in 9%Cr low activation martensitic steels”, *New Developments on Metallurgy and Applications of High Strength Steels*, (Proc. Int. Conf. Buenos Aires 2008), TMS Publishing Company, Warrendale (2008) 331-342.